Optical studies of transparent ferroelectric strontium–barium niobate/silica nanocomposite

S. G. Lu, C. L. Mak,[a] and K. H. Wong
Department of Applied Physics and Materials Research Centre, The Hong Kong Polytechnic University, Hung Hom, Kowloon, Hong Kong, People's Republic of China

(Received 28 January 2003; accepted 20 June 2003)

Transparent ferroelectric strontium–barium niobate (SBN) doped silica nanocomposites were prepared via a modified sol–gel process. Their structural properties were characterized by x-ray diffraction and Raman spectroscopy. It was found that by annealing the nanocomposites at temperatures between 600 and 800 °C, pure tetragonal tungsten bronze phase SBN crystallites with sizes ranging from 8 to 23 nm were obtained. Differential scanning calorimetry measurement has indicated that nanometer size ferroelectric SBN has a reduced phase transition temperature compared with that of bulk SBN. Photoluminescence and optical transmission studies of these composites have revealed noticeable blueshifts in the emission band peak and the absorption edge, respectively. The refractive index of the nanocomposite annealed at 700 °C was measured by ellipsometry. The value obtained is larger than that of pure sol–gel derived silica but smaller than that of SBN crystal, and can be described by the Bruggeman effective medium approximation. [DOI: 10.1063/1.1599047]

I. INTRODUCTION

Ferroelectric strontium–barium niobate (SBN) is the subject of numerous studies[1–4] due to its large dielectric constant, electro-optical coefficient, pyroelectric coefficient, and lead free composition. Nanocomposites formed by dispersing nanometer size SBN particles in transparent solid matrices are expected to be useful in optical applications, such as optical filter, optical communication, and computing devices.[5] These nanocomposite systems have also been used to investigate the size effect in ferroelectric materials.[6–10] Optical studies, of them, however, are sparse. This may be due to the difficulties in fabricating transparent nanocomposites.

Among the different transparent solid matrices, silica has emerged as one with good potential for device application. It has high transmission efficiency from the visible to deep UV, so that wideband applications are possible. Besides, silica has a high threshold for photo- and thermal degradation. It produces no apparent darkening or semipermanent damage under high intensity irradiation. The sol–gel process, on the other hand, is one of the promising methods for preparing ferroelectric nanoparticles. Advantages of the sol–gel process include low processing temperature, ease of chemical composition control, excellent homogeneity, high reproducibility, low equipment cost, and simple procedure. In addition, the particle size of a ferroelectric nanopowder can be easily controlled by varying the calcination temperature.

Preparation of transparent ferroelectric nanocomposites via sol-gel has several inherent problems. They are (1) different hydrolyzing speeds of ferroelectric and matrix precursor sols resulting in precipitation of the ferroelectric precursor; (2) high annealing temperature to form a ferroelectric crystalline structure resulting in the disappearance of vitrification of a clear glass matrix; and (3) the existence of impurity phases. In this article, we have prepared transparent ferroelectric SBN/SiO_2 nanocomposites via a modified sol–gel process. X-ray diffraction (XRD) and Raman spectroscopy were used to study the structural properties of these nanocomposites. The ferroelectric-to-paraelectric phase transition of the doped SBN nanoparticles was studied by differential scanning calorimetry (DSC) while the energy structure of the nanocomposites was investigated by photoluminescence studies. Finally, the optical properties of these nanocomposites were investigated by ellipsometry and transmittance measurements.

II. EXPERIMENT

Metallic strontium and barium were individually dissolved in 2-methoxyethanol to form Sr and Ba alkoxides, respectively. Niobium alkoxide was obtained by reacting $NbCl_5$ with KOH using 2-methoxyethanol as the solvent. The three metal alkoxides were mixed and refluxed to form SBN sol of desired concentration and stoichiometric ratio $(Sr/Ba=1)$. The sol was then blended with tetraethylorthosilicate (TEOS) and hydrolyzed with HC*l* to enhance the gelation speed. The *p*H value of the final sol was kept at $\sim 2-3$. To prevent the precipitation of SBN particles, excess 2-methoxyethanol was used as the peptizing agent. The mixed sol was placed at room temperature for 10 days to become a stiff gel. The gel was then dried at 60 °C for another 10 days. Finally, the as-prepared gel was annealed at temperatures between 600 and 800 °C for different durations. Using Achimedes' method, the density of SBN/SiO_2 was determined to be $1.8\,g/cm^3$ which is less than that of bulk SBN

[a]Electronic mail: apaclmak@polyu.edu.hk

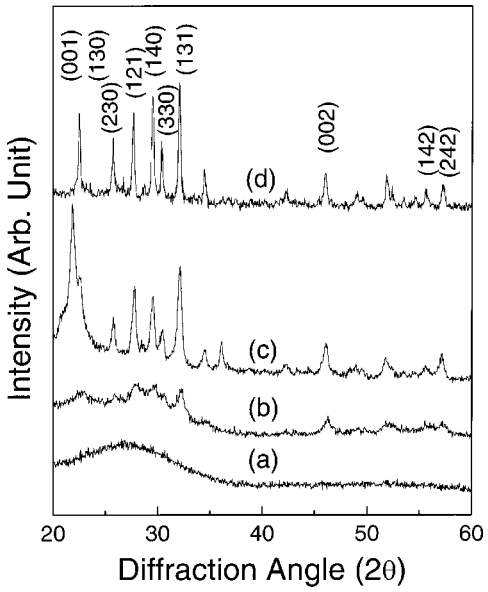

FIG. 1. XRD profiles of SBN/SiO_2 nanocomposites annealed at (a) 600 °C: amporphous state, transparent; (b) 700 °C: TTB phase crystallite state, transparent; (c) 800 °C: TTB phase crystallite state, opaque, and (d) sol–gel derived SBN powder.

$(5.4\,g/cm^3)$ as well as fuse glass $(2.2\,g/cm^3)$, [11] but larger than that of our undoped sol–gel silica glass annealed at 700 °C $(1.56\,g/cm^3)$.

III. RESULTS AND DISCUSSION

XRD profiles of the SBN doped nanocomposites were measured by an x-ray diffractometer (Philips X'pert) and are shown in Fig. 1. The diffraction peaks coincide well with those of sol–gel derived SBN powder indicating that the embedded SBN crystallites have a pure tetragonal tungsten bronze (TTB) structure. The broad diffraction peaks [Fig. 1(b)] suggest that the crystallites are very small indeed. After subtracting instrumental broadening, the average crystallite size is estimated in accordance with the Scherrer formula.[12] The (131) plane diffraction peak was used to estimate the crystallite size because of its strong intensity. Upon increasing the annealing temperature, the diffraction peaks became narrower and stronger, indicating the presence of bigger SBN crystallites. Consequently the composite became opaque to visible light. On the contrary, if we lowered the annealing temperature, the composite was transparent. No x-ray diffraction peak, however, was observed. This means that the embedded SBN was mainly amorphous. From our studies, a temperature window between 700 and 750 °C is obtained. As-prepared samples annealed within this temperature window for 2 h show a prominent presence of TTB phase SBN as well as a high optical transparency.

The Raman spectra were obtained by excitation with 514.5 nm laser light from a continuous wave (cw) argon gas laser (Coherent Innova 70). The power was kept at 50 mW to avoid laser annealing of the samples. A 55 mm *f*/1.8 lens was used to collect scattered light which was dispersed and detected using a double grating spectrometer (SPEX 1403) equipped with a cooled photomultiplier tube (Hamamatsu R943-2). As expected, one can observe that the intensity of the SBN/SiO_2 spectrum was weaker than that of the single crystal. Apart from the intensity, the two spectra look very similar with characteristic peaks[13] at 251 and 642 cm^{-1}, as shown in Fig. 2. Beside these two peaks, no other peak was observed, indicating that no impurity but pure TTB SBN phase existed.

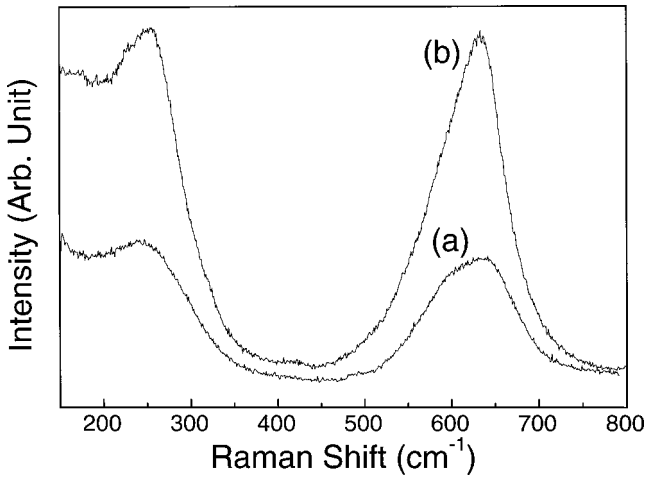

FIG. 2. Raman spectra of (a) SBN/SiO_2 nanocomposites annealed at 700 °C and (b) SBN single crystal.

The ferroelectric-to-paraelectric phase transition of the embedded SBN in the SBN/silica nanocomposite was investigated by a DSC (Perkin-Elmer DSC7). The phase transition peak is broad and weak as shown in Fig. 3. This is primarily the result of the small crystallite size and low concentration of the embedded SBN. In our experiments, the mole percentage of SBN was fixed at 8% by controlling the mole ratio of the TEOS and SBN sol used. Experimentally, the specific heat is calculated from the heat flow, so the heat flow peak actually reflects the phase transition that occurs in the materials. This result means that the phase transition in nanometer size SBN has a very small energy change. And the average transformation temperature is at about 50 °C, that is, ~70 °C lower than that of the SBN single crystal (120 °C for SBN50

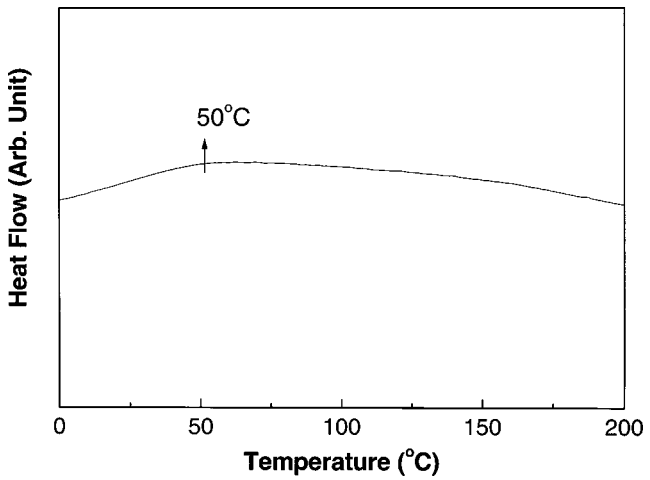

FIG. 3. DSC thermogram heating rates of 10 °C/min for a SBN50/silica nanocomposite.

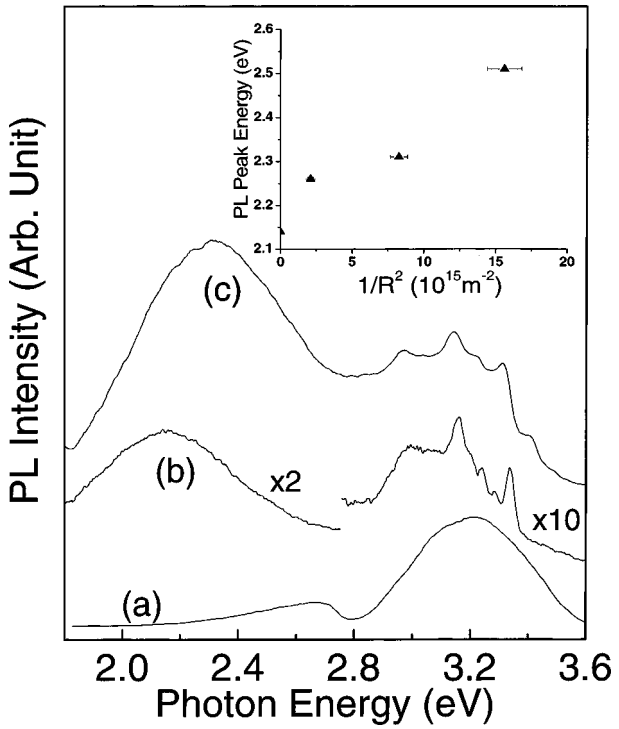

FIG. 4. Photoluminescence spectra measured at 11 K of (a) sol–gel silica, (b) single crystal SBN, and (c) SBN/SiO_2 nanocomposites with crystallite size of 11 nm. The inset shows the dependence of the PL peak energy as a function of the SBN crystallite size.

single crystal[14]). This result is consistent with that obtained in the sol–gel derived ultrafine SBN powders.[4] Based on our XRD, Raman, and DSC results, we conclude that TTB phase SBN crystallites were dispersed into the SiO_2 matrix via this modified sol–gel process.

Refractive indices of the nanocomposites (annealed at 700 °C) and pure silica gel glass were obtained by an ellipsometer (Jobin-Yvon, UVISEL). Using the Bruggeman effective medium approximation (EMA),[15] the refractive index of the nanocomposites, n, can be approximated by

$$f\frac{n_2^2-n^2}{n_2^2-2n^2}+(1-f)\frac{n_1^2-n^2}{n_1^2-2n^2}=0, \tag{1}$$

where n_1 and n_2 are the refractive indices of silica and SBN, respectively, and f is the volume fraction of the embedded SBN. Taking the mole percent of SBN crystallite in our nanocomposites to be 8%, and the densities of SBN and silica to be 5.4 and 1.56 g/cm^3, respectively, we derive the volume fraction of SBN in the nanocomposites to be 14%. Assuming the refractive indices of SBN bulk material and pure silica at 2.48 eV to be 2.354 and 1.468, respectively,[16] the estimated refractive index of our nanocomposites is $\sim$1.85. This value is slightly larger than our measured value of 1.65. The discrepancy may be ascribed to the fact that we did not take into account of the porosity of the sample in our calculations.

Figure 4 shows the photoluminescence (PL) spectra measured at 11 K for our nanocomposites of different SBN crystallite size. In general, the nanocomposites consist of two strong emission bands located at $\sim$3.2 and $\sim$2.3 eV. The

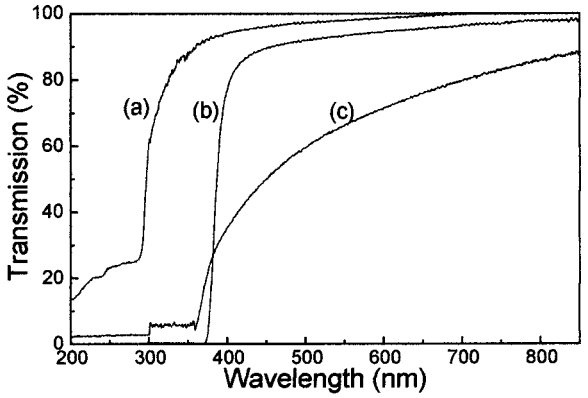

FIG. 5. Transmission spectra of (a) sol–gel silica, (b) a SBN single crystal, and (c) a SBN/SiO_2 nanocomposite with crystallite size of 11 nm.

first band has a broad profile superimposed by sharp peaks. The broad profile originates from sol–gel silica. It can be attributed to carbon impurity, an –O–O-type defect, an O_2^- intrinsic defect, and an irradiation induced intrinsic defect.[17] The position of this peak, as expected, is independent of the embedded SBN crystallite size. The sharp peaks, on the other hand, originate from SBN crystals. Compared with those from SBN single crystal, these peaks from nanocomposites are much stronger. The enhancement is probably due to the resonance effect that arises from the intense 3.2 eV emission band of the sol–gel silica. This emission band is close to the measured absorption edge of embedded SBN (Fig. 5). The size of the embedded SBN nanocrystals, however, has no effect on the position of these peaks. Since Sr^{2+}, Ba^{2+}, and Nb^{5+} ions have electron configurations of $(4s^24p^6)$, $(5s^25p^6)$, and $(4s^24p^6)$, respectively, i.e., the outermost electrons are p electrons, these transitions are unlikely to be caused by crystal field splitting of the multiplets of Sr^{2+}, Ba^{2+}, and Nb^{5+}. We suggest that these transitions may be related to the transition between the Nb^{4+} polaron state and the valence band.[18] The 2.65 eV emission band of the pure sol–gel silica may be related to the triplet to ground state transition of neutral oxygen vacancy defects.[19] In our nanocomposites, a more dominant band at 2.3 eV from SBN crystal was observed. This band has a very large full width at half maximum (FWHM) and becomes narrower for smaller SBN crystallites. Additionally, the peak position shifts towards higher energy with a decrease in crystallite size. The inset shows the dependence of this peak energy as a function of the inverse square of the mean radius of the SBN particle. The energy seems to vary as the inverse square of the dimension, as predicted by the effective mass approximation.[20]

Transmission studies were carried out over the wavelength range of 200-850 nm using an UV-visible scanning spectrophotometer (Shimadzu, UV-2101). Figures 5(a)–5(c) show the transmission spectra of the undoped silica, SBN single crystal, and SBN doped nanocomposites, respectively. For the SBN nanocomposite sample 0.64 mm thick, the optical transmission is about 70% in the visible range. This is comparable with that of SBN thin film.[1] Figure 6 shows a photograph of a typical SBN doped nanocomposite having good transparency. From the transmission spectra shown in

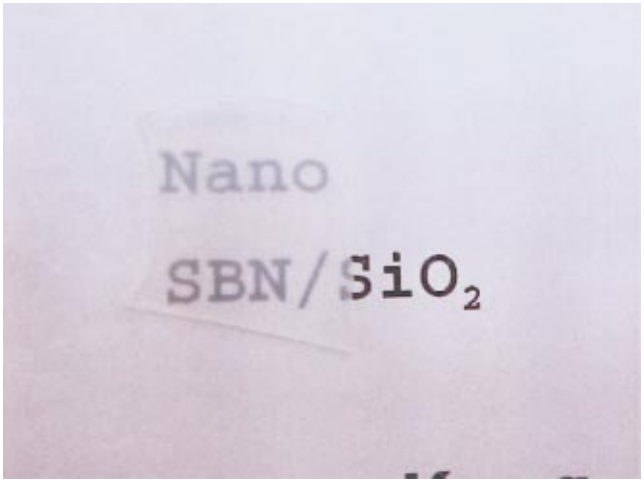

FIG. 6. (Color) Photograph showing a SBN/SiO_2 nanocomposite with good transparency.

Fig. 5, two absorption edges, located at about 300 and 360 nm, are observed. They are related to the absorption edges of the SiO_2 matrix and the embedded SBN, respectively. Previous studies assigned the absorption edge of SBN to charge transfer within the niobate complex.[21] Under excitation by light, the electrons are excited from the valence band, which is made up of molecular orbitals localized at O^{2-} ions, towards the t_{2g} orbitals in the conduction band. This conduction band, on the other hand, is from one of the least filled molecular orbitals localized mainly at Nb^{5+} ions. This absorption edge shows a large blueshift as the SBN crystallite size decreases. Furthermore, no absorption band was found around 650 nm, which indicates that the 2.3 eV luminescence band in Fig. 4 is unlikely to be caused by the transition of unwanted Cr^{3+} in the SBN crystal due to trace amounts of Cr at the ppm level.[22]

In order to estimate the energy band gap of the SBN crystallites, we converted the absorption spectra into normalized absorption coefficient spectra, shown in Fig. 7. It is well known that there are two types of fundamental optical transition, namely, direct and indirect. For a direct transition, the absorption coefficient α is proportional to $(h\nu - E_g)^{1/2}$, where E_g is the energy band gap and $h\nu$ is the incident photon energy. For an indirect transition, on the other hand, the absorption coefficient is proportional to $(h\nu - E_g \pm E_p)^2$, where E_p is the phonon energy, and the plus and minus signs represent jumps related to phonon absorption and emission, respectively. In general, the absorption coefficient in an indirect jump is less than $10^3\ cm^{-1}$. [23,24] From Fig. 7, we notice that our measured absorption coefficients are less than $10^3\ cm^{-1}$ and the curves have good linear relations. All these facts indicate that the absorption in our samples is from an indirect transition. In comparing with the absorption curve of undoped silica, the profiles with energy above 3.5 eV are mainly due to the silica matrix. Below 3.5 eV, there are two linear and one nonlinear regions. They correspond to the slow-dropping (I: weak absorption), shoulder (II), and fast-dropping (III: strong absorption) regimes. These observations are in agreement with the characteristics of the absorption edges of $LiNbO_3$ (LN) crystals.[24] Similar to LN, the slow-dropping part (part I) comes from the contribution of impurities and defects. The fast-dropping part (part III) is assigned to indirect transitions. For indirect transition, the $\alpha^{1/2}$ vs $h\nu$ curve should contain two linear parts, which correspond to photon energies $>(E_g - E_p)$ and $(E_g + E_p)$. However, our measurement shows a single linear part only, due to limited resolution. In order to estimate the relative shift in E_g, we consider the fast-dropping part (part III) to be represented by $h\nu - (E_g + E_p)$. By assuming the indirect transitions of SBN single crystal and SBN nanocomposites are due to the contribution of the same phonon (i.e., same E_p value), we can obtained the relative shift of the effective band gap with respect to the bulk SBN single crystal. The inset of Fig. 7 shows the relative shift as a function of the crystallite size. Our results demonstrate that the band gap energy increases with a decrease of SBN crystallite size. These transmittance measurements further confirm that quantum confinement has occurred in nanometer size ferroelectric crystallites.

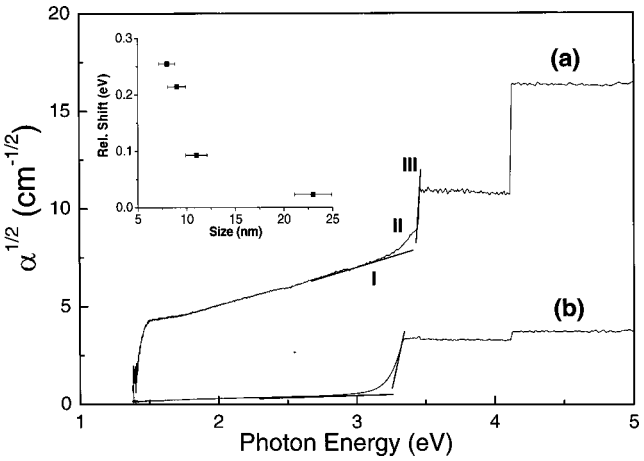

FIG. 7. Normalized absorption spectra of (a) a SBN/SiO_2 nanocomposite with crystallite size of 11 nm and (b) a SBN single crystal.

IV. CONCLUSION

We have fabricated transparent ferroelectric nanocomposites based on dispensing SBN nanoparticles within pores of sol–gel silica. The structural properties of tetragonal tungsten bronze phase SBN obtained was confirmed by x-ray diffraction and Raman spectroscopy. Photoluminescence studies revealed an emission band at 2.3 eV due to transitions within the NbO_6 complex of SBN crystallites. An increase in blueshift with a decrease in SBN crystallite size was observed. Transmittance measurements showed that the absorption edges of SBN crystallites were also blueshifted. Similar to those observed in photoluminescence spectra, the amount of these shifts increased substantially with a decrease in crystallite size. This demonstrates that the energy structure of nanoferroelectric materials has a strong dependence on the crystallite size.

ACKNOWLEDGMENTS

This work was supported by the Research Grant Council of the Hong Kong Special Administrative Region (PolyU5291/02P) and the Center of Smart Materials of the Hong Kong Polytechnic University . The authors are grateful to H. K. Hui for assistance in the preparation of samples, and Dr. Y. L. Zhang for providing SBN single crystals.

[1] Y. Xu, C. J. Chen, R. Xu, and J. D. Mackenzie, Phys. Rev. B **44**, 35 (1991).
[2] R. Guo A. S. Bhalla, G. Burns and F. H. Dacol, Ferroelectrics **93**, 397 (1989).
[3] C. H. Luk, C. L. Mak, and K. H. Wong, Thin Solid Films **298**, 57 (1997).
[4] S. G. Lu, C. L. Mak, and K. H. Wong, J. Am. Ceram. Soc. **84**, 79 (2001).
[5] R. E. Newnham, Adv. Ceram. Mater. **3**, 12 (1988).
[6] K. Ishikawa, K. Yoshikawa, and N. Okada, Phys. Rev. B **37**, 5852 (1988).
[7] S. G. Lu, H. L. Liu, Y. Han, L. Y. Zhang, and X. Yao, Ferroelectr. Lett. Sect. **18**, 115 (1994).
[8] S. Chattopadhyay, P. Ayyub, V. R. Palkar, and M. Multani, Phys. Rev. B **52**, 13177 (1995).
[9] M. H. Frey and D. A. Payne, Phys. Rev. B **54**, 3158 (1996).
[10] D. McCauley, R. E. Newnham, and C. A. Randall, J. Am. Ceram. Soc. **81**, 979 (1998).
[11] P. W. McMillan, Glass Ceramics, 2nd ed. (Academic, London, 1979), p. 159.
[12] Handbook of X-Rays, edited by E. F. Kaelble (McGraw–Hill, New York, 1967), p. 17.
[13] E. Amzallag, T. S. Chang, and R. H. Pantell, J. Appl. Phys. **42**, 3254 (1971).
[14] A. M. Glass, J. Appl. Phys. **40**, 4699 (1969).
[15] D. A. G. Bruggeman, Ann. Phys. (Leipzig) **24**, 636 (1935).
[16] Landolt-Bornstein, Numerical Data and Functional Relationships in Science and Technology, New Series Group III, Vol. 16 Ferroelectric and Related Substances, Subvolume a: Oxides, (1981), p. 535.
[17] M. A. Garcia, S. E. Paje, M. A. Villegas, and J. Llopis, Mater. Lett. **43**, 23 (2000).
[18] M. Gao, R. Pankrath, S. Kapphan, and V. Vikhnin, Appl. Phys. B: Lasers Opt. **B68**, 849 (1999).
[19] M. A. S. Kalceff and M. R. Philips, Phys. Rev. B **52**, 3122 (1995).
[20] L. E. Brus, J. Chem. Phys. **80**, 4403 (1984).
[21] A. Kh. Zeinally, N. N. Lebedeva, A. R. Mordukhayev, and M. A. Osman, Ferroelectrics **45**, 83 (1982).
[22] S. G. Lu, C. L. Mak, K. H. Wong, and K. W. Cheah, Appl. Phys. Lett. **79**, 4310 (2001).
[23] Solid State Physics, edited by J. X. Fang and D. Lu (Shanghai Science and Technology Press, Shanghai, 1981).
[24] S. M. Liu, G. Y. Zhang, and J. B. Guo, Acta Phys. Sin. **35**, 1357 (1986).